Front. Electr. Electron. Eng. China 2007, 2(4): 425–431
DOI 10.1007/s11460-007-0079-7

RESEARCH ARTICLE

**ZHOU Yangzhong, HU Yuwen, HUANG Wenxin, ZHONG Tianyun**

# Research on a direct torque control for an electrically excited synchronous motor drive with low ripple in flux and torque



**Abstract** The electrically excited synchronous motor (ESM) has typically small synchronous inductance values and quite low transient values because of the damper windings mounted on the rotor. Therefore, the torque and stator flux linkage ripples are high in the direct torque control (DTC) drive of the ESM with a torque and flux linkage hysteresis controller (basic DTC). A DTC scheme with space vector modulation (SVM) for the ESM was investigated in this paper. It is based on the compensation of the stator flux linkage vector error using the space vector modulation in order to decrease the torque and flux linkage ripples and produce fixed switching frequency under the principle that the torque is controlled by the torque angle in the ESM. Compared with the basic DTC, the results of the simulation and experiment show that the torque and flux linkage ripples are reduced, the maximum current value is decreased during the startup, and the current distortion is much smaller in the steady-state under the SVM-DTC. The field-weakening control is incorporated with the SVM-DTC successfully.

**Keywords** synchronous machines, electrically excited synchronous motor, direct torque control, space vector modulation, field weakening

## 1 Introduction

In the late 1990s, the techniques of the direct torque control (DTC) for the permanent synchronous motor (PMSM) were presented by Rahman and Hu [1], and the DTC theories for the electrically excited synchronous motor (ESM) were studied partly by Finnish researchers in about 1998 [2,3]. When compared with the asynchronous motor (AM), the inductance value of the ESM is small, and the dynamic inductance value is even lower in the ESM due to the damper windings in the rotor. The ripples in the torque and stator flux linkage may be high, and the stability of the drive system may be affected if the basic DTC with stator flux linkage and torque hysteresis controllers is applied into the ESM. In order to decrease these ripples, a number of feasible methods were investigated for AM and PMSM drives. Recently, many researchers have been making efforts on the DTC scheme with SVM. For example, in Ref. [4], a flux linkage closed SVM-DTC control scheme for AM was presented, in which the stator and rotor flux linkage were estimated under the knowledge of motor inductance parameters and the rotation coordinate conversion. The papers [5–7] investigated a torque closed SVM-DTC scheme based on the one-step anticipation for stator flux linkage vector and the idea that the torque can be controlled with the torque angle. In Ref. [8], a torque and stator flux linkage closed SVM-DTC scheme was presented in a Clark frame based on stator flux linkage orientation, but the rotation frame conversion was demanded. Reference [9] presented a mathematical model based SVM-DTC control scheme, but a quadrature equation should have been resolved. Many other SVM-DTC schemes were also studied in Refs. [10–14]. From the above reviews, although many SVM-DTC schemes were investigated intensively for AM and PMSM, the SVM-DTC scheme for the ESM has not been fully presented.

Many ESMs are being used in different industries because of their advantages such as good dynamic performance, adjustable power fact, and high efficiency. Thus, it is very valuable to research the ESM SVM-DTC. Although the ESM and the PMSM are all SMs, the excited winding and damper windings mounted on the ESM rotor make the ESM torque control principle different from that of the PMSM. Therefore, it is very necessary to research the ESM SVM-DTC.

After defining the new torque angle, this paper displays a modified SVM-DTC scheme for the ESM based on the principle that the torque is controlled by the torque angle in order to decrease the ripples of torque and stator flux linkage. The weakening field method is incorporated into the modified SVM-DTC, and the working range of speed is increased.

Translated from *Proceedings of the Chinese Society for Electrical Engineering*, 2006, 26(7): 152−157 [译自: 中国电机工程学报]

ZHOU Yangzhong (✉), HU Yuwen, HUANG Wenxin, ZHONG Tianyun
Department of Electrical Engineering, Huaiying Institute, Huai'an 223001, China
E-mail: zhty_75313@sina.com

## 2 Torque and stator flux linkage control principle in SVM-DTC

The whole mathematical model of torque for the ESM with field winding and damper windings was investigated in Ref. [15], which expressly shows that the electric magnetic torque is comprised of the main torque $T_{e_1}$, which is produced by the multi-effect between the field winding flux linkage and the stator winding flux linkage, and the adjective torque $T_{e_2}$, which is generated by the multi-effect between the damper winding flux linkage and stator winding flux linkage. $T_{e_1}$ and $T_{e_2}$ are expressed as

$$T_{e_1} = \frac{3p\varphi_s}{4L_dL_q}[2M_{sf}i_fL_q\sin\delta - \varphi_s(L_q - L_d)\sin 2\delta] \quad (1)$$

$$T_{e_2} = -\frac{3}{2}p\varphi_s\left(-\frac{M_{sD}}{L_d}i_D\sin\delta + \frac{M_{sQ}}{L_q}i_Q\cos\delta\right) \quad (2)$$

where $\delta$ is the angle between the stator flux linkage vector and the rotor $d$-axis, $p$ is the pole pairs, $\varphi_s$ is the modulus of the stator flux linkage, $i_f$, $i_D$ and $i_Q$ are the rotor field current, the $d$-axis and $q$-axis damper winding current respectively, $M_{sf}$, $M_{sD}$ and $M_{sQ}$ are the multi-inductance between the stator winding and rotor field winding, the $d$-axis and $q$-axis damper winding, respectively, $L_d$ and $L_q$ are stator $d$-axis and $q$-axis inductance, respectively.

If we define the angle between the stator flux linkage vector and the air gap flux linkage, e.g. $\theta$ as the torque angle, the whole torque produced by the multi-effect among the field magnet, the damper winding magnet and the stator winding magnet is the cross product of the air gap flux linkage and the stator flux linkage

$$T_e = \frac{3}{2L_{s\sigma}}p\varphi_s\times\varphi = \frac{3}{2L_{s\sigma}}p|\varphi_s||\varphi|\sin\theta \quad (3)$$

where $\varphi_s$ and $\varphi$ represent the stator and the air gap flux linkage vector, respectively, and $L_{s\sigma}$ is the stator leakage inductance.

It has been verified that the air gap flux linkage time constant is larger than 10ms due to the damping effect of the damper winding. The time constant is even larger than the system sampling period, and thus the space position of the air gap flux linkage vector in the $d$-$q$ rotation frame is almost not changed in dynamic state. Thus, the electric magnetic torque can be controlled by the torque angle $\theta$ using the stator flux linkage vector rotation.

Figure 1(a) shows the torque control diagram in the SVM-DTC system, neglecting the stator winding resistance and assuming that the stator flux linkage vector is $\varphi_{sk}$ when the $k$th sampling period is over. The control reference stator flux linkage vector $\varphi_{sk+1}$ is anticipated with torque error, e.g. ($T_e^* - T_e$) and the given stator flux linkage modulus $\varphi_s^*$. The stator flux linkage error vector $\Delta\varphi_{se}$ can be calculated from $\varphi_{sk+1}$ and the actual stator flux linkage vector $\varphi_{sk}$. The $\boldsymbol{V}_6$, $\boldsymbol{V}_2$ and $\boldsymbol{V}_0$ voltage vector keep working with $T_1$, $T_2$ and $T_0$ ($T_0 = T_s - T_1 - T_2$), respectively, in order to cancel the stator flux linkage error vector $\Delta\varphi_{se}$. Thus, the torque and stator flux linkage vector are controlled accurately and quickly. Figure 1(b) shows the stator flux linkage vector envelope curves of the basic DTC and SVM-DTC. The ripples of the stator flux linkage and the torque in the basic DTC is large because the system adopts the flux linkage and the torque hysteresis controllers while only one voltage vector is selected during each sampling period. However, the ripples of the stator flux linkage and the torque is low in the SVM-DTC system as a result that this system can output many voltage vectors in one sampling period by means of the SVM technique, and consequently the stator flux linkage modulus can be controlled accurately.

## 3 Modeling results

The motor parameters used in the simulation are shown in Table 1. Two Matlab/Simulink models were developed to examine the different control algorithms. One is for the basic DTC ESM system and another for the SVM-DTC ESM system. In the simulation, the sampling interval is 100 μs for the two systems. Figure 2 is the SVM-DTC system diagram.

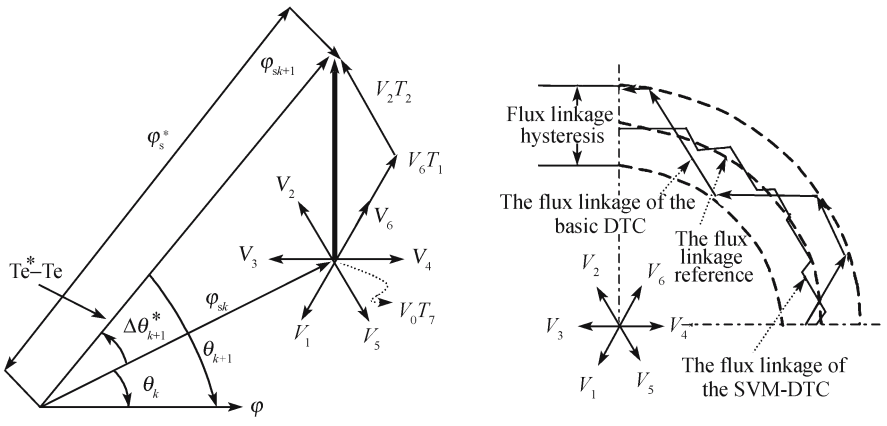


**Fig. 1** The control principle for the torque and the stator flux linkage
(a) Torque control; (b) the flux linkage vector envelope curves

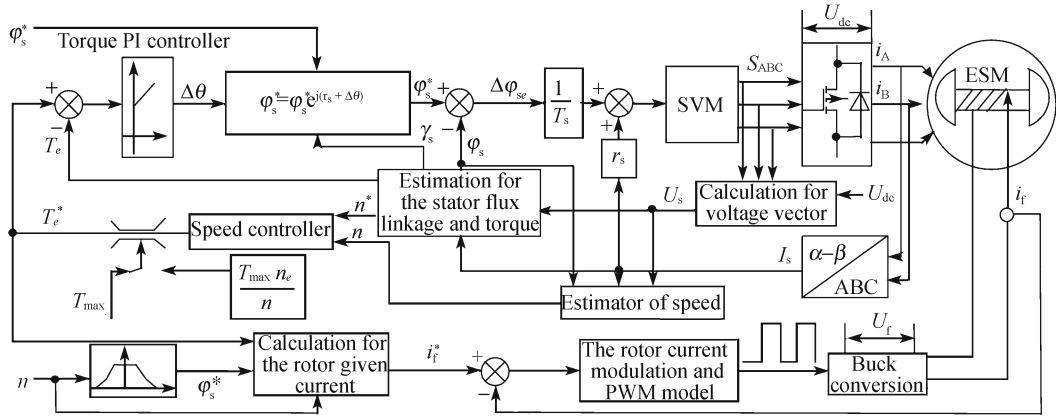


**Fig. 2** System diagram of the SVM-DTC

**Table 1** Date of motor

| | |
|---|---|
| Nominal power | 300 W |
| Nominal voltage | 220 V |
| Nominal speed | 1 500 r/min |
| Pole pairs | 2 |
| *d*-axis inductance | 0.9247 H |
| *q*-axis inductance | 0.604 H |
| Multi-inductance of stator and rotor | 0.45 H |
| Stator resistance | 13.3 Ω |
| Rotor resistance | 9.8 Ω |
| Stator leakage inductance | 0.1 H |
| Rotor excited winding self inductance | 0.4324 H |
| Self inductance of *d*-axis damper winding | 0.00356 H |
| Resistance of *d*-axis damper winding | 0.151 Ω |
| Multi-inductance of *d*-axis damper winding and excited winding | 0.028308 H |
| Multi-inductance of *d*-axis damper winding and stator winding | 0.04236 H |
| Self inductance of *q*-axis damper winding | 0.0032 H |
| Resistance of *q*-axis damper winding | 0.14 Ω |
| Multi-inductance of *q*-axis damper winding and stator winding | 0.031222 H |

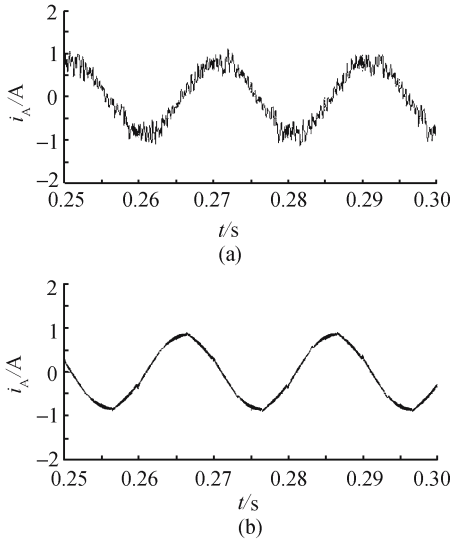


**Fig. 3** Simulation waveforms of phase current at 1 500 r·min$^{-1}$ with 0.5 N·m load

(a) Basic DTC; (b) SVM-DTC

The field current is controlled by using a buck conversion. The output variable of the torque PI controller is the stator flux linkage vector rotational angle $\Delta\theta$.

In this paper, zero voltage vector $\boldsymbol{V}_0$ is inserted in the middle of every sampling period, and the two active voltage vectors $\boldsymbol{V}_1$, $\boldsymbol{V}_2$ are output at the beginning and the end of every sampling period symmetrically.

Figure 3 shows the steady-state current of two systems with 0.5 N·m load. From the results shown in Fig. 3, it is seen that the current waveform in the SVM-DTC is much smoother than that of the basic DTC.

Figure 4 shows the steady-state torque and stator flux linkage of the two systems at the nominal speed with 0.5 N·m load and nominal stator flux linkage 0.61 Wb. The ripples of the torque and the stator flux linkage are $\pm$0.5 N·m and $\pm$0.03 Wb, respectively, under the basic DTC drive. However, the ripples under the SVM DTC are only $-0.1-0.15$ N·m and 0.005 Wb, respectively. Therefore, the developed torque and the stator flux linkage of the SVM-DTC possess fewer ripples than those of the basic DTC.

In Fig. 5, comparisons are made between the torque dynamic performances of the two algorithms. It is seen that the response time of the SVM-DTC drive is almost the same as that of the basic DTC drive.

From the results shown in Figs. 3 and 4, it is seen that the steady-state performance of the SVM-DTC is much better than that of the basic DTC. For dynamic performance, the SVM-DTC is almost as good as the basic DTC.

## 4 Experimental results

The motor parameters used in the experiment are shown in Table 1. The sampling period is 100 μs in the basic DTC and the SVM-DTC. The diagram of the SVM-DTC with sensorless technique is shown in Fig. 2.

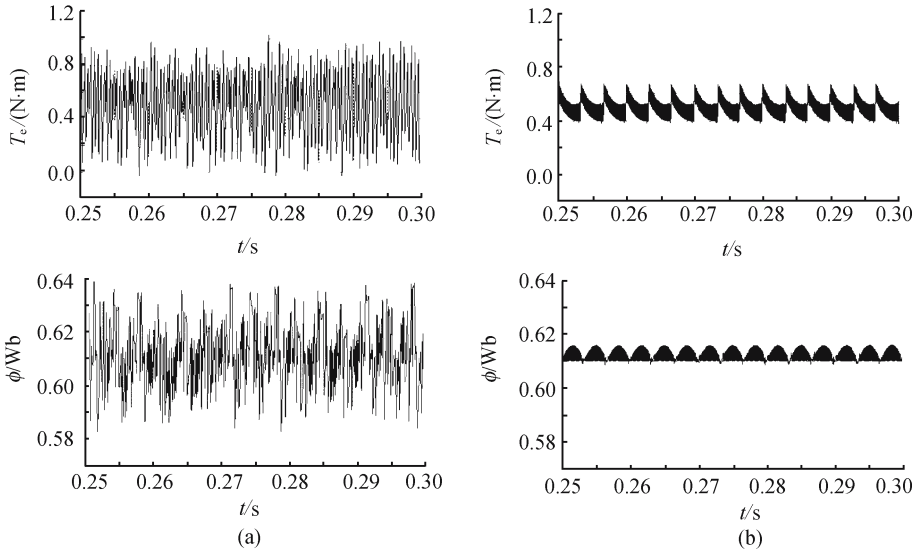


**Fig. 4** Simulation waveforms of torque and stator flux linkage at 1 500 r/min with 0.5 N·m load
(a) Basic DTC; (b) SVM-DTC

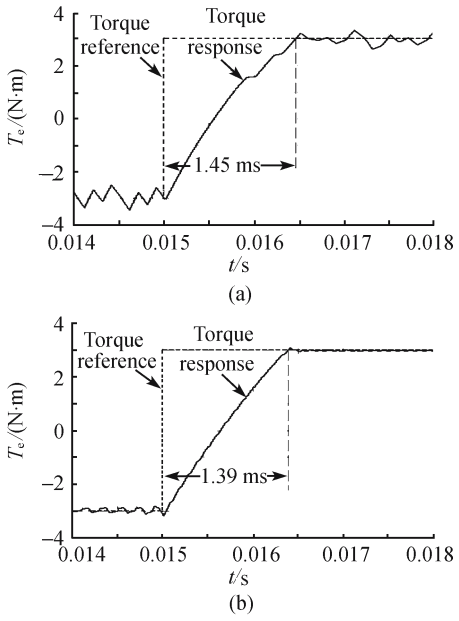


**Fig. 5** Simulation waveforms of the torque step response
(a) Basic DTC; (b) SVM-DTC

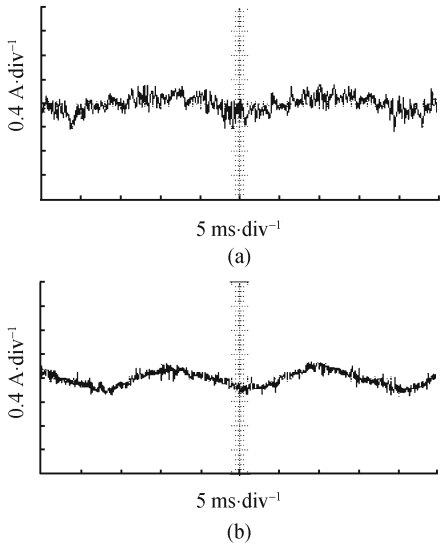


**Fig. 6** Experimental waveforms of phase current at 1 500 r/min with no load
(a) Basic DTC; (b) SVM-DTC

The steady-state phase currents of the two DTC schemes are shown in Fig. 6. The current waveform of the SVM-DTC is smoother than that of the basic DTC.

The steady-state torque and the stator flux linkage waveforms of the two schemes at nominal speed with no load are shown in Fig. 7. The ripples of the torque and the stator flux linkage of the basic DTC are $\pm 1$ N·m and $\pm 0.025$ Wb, respectively. However, the ripples of the SVM-DTC are only $\pm 0.5$ N·m and $\pm 0.005$ Wb.

In Fig. 8, the steady-state torque and the stator flux linkage waveforms at 200 r/min speed with no load are shown. From the results displayed in Fig. 8(a) and (b), we can discover that the ripples of the torque and the stator flux linkage of the SVM-DTC are all lower than those of the basic DTC. Moreover, at other speeds, similar conclusions can be obtained.

The start-up torque and current responses with no load and limited 3 N·m are shown in Fig. 9. The ripple of the torque and the maximal value of current in the basic DTC are $\pm 1.6$ N·m and 3.2 A, respectively. However, these values are only $\pm 0.8$ N·m and 2.2 A, respectively, in the SVM-DTC. From the above experimental results, we can see that the start-up current is much decreased and the start-up operation is very smooth in the SVM-DTC drive due to the exact control of the torque and the stator flux linkage.

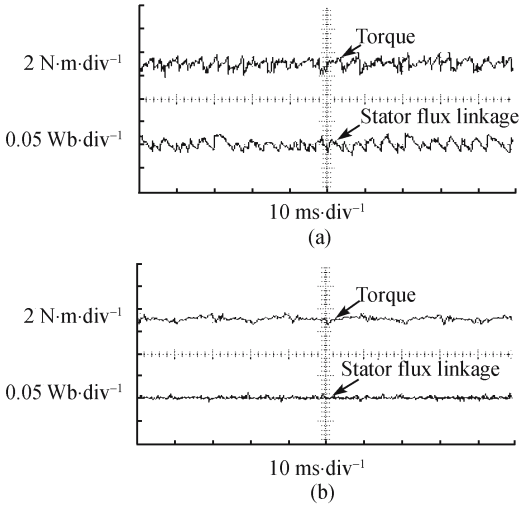


**Fig. 7** Experimental waveforms of torque and stator flux linkage at 1 500 r·min$^{-1}$ with no load
(a) Basic DTC; (b) SVM-DTC

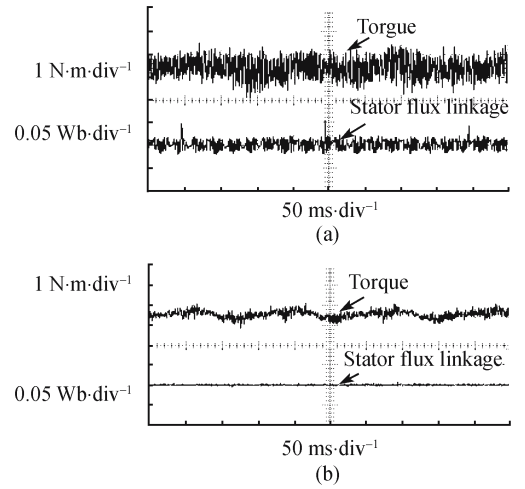


**Fig. 8** Experimental waveforms of the torque and the stator flux linkage at 200 r/min with no load
(a) Basic DTC; (b) SVM-DTC

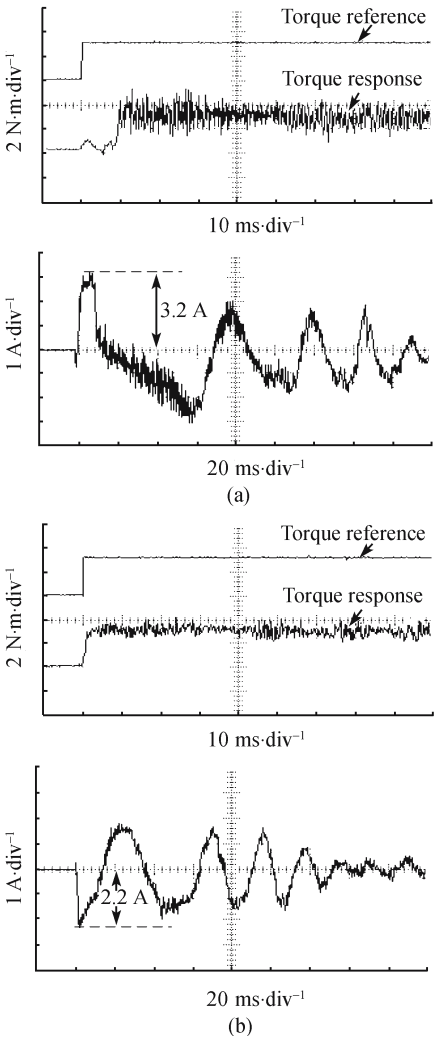


**Fig. 9** Experimental waveforms of the torque and the phase current during the startup from standstill with no load
(a) Basic DTC; (b) SVM-DTC

In Fig. 10, the torque dynamic responses of the two DTC schemes from −3 to +3 N·m are researched. The torque response time of the SVM-DTC drive is almost the same as that of the basic DTC drive, which is the same with the simulation.

From the above experimental results, it is seen that the ripples of the torque and the stator flux linkage in the basic DTC are all fewer than those in the SVM-DTC, and the start-up maximal value of the current in the SVM-DTC is much more decreased compared with that in the basic DTC.

## 5 Field weakening

The field weakening control is included in the SVM-DTC to increase the range of speed. Here, the speed is limited to 2 000 r/min due to the limited maximum speed of the motor.

The rotor excited current control scheme with unit inner power fact is applied below the nominal speed in order to reduce the loss of rotor resistance, while the rotor field current control scheme with unit outer power fact used over the nominal speed to increase the load ability in the weakening range. According to the DTC control features, the relationship between the rotor field current, the torque, and the stator flux linkage modulus under the condition of unit outer power fact is given as

$$i_{\mathrm{f}}=\frac{(3p\varphi_{\mathrm{s}})^2+4L_dL_q\left(\dfrac{T_e}{\varphi_{\mathrm{s}}}\right)^2}{3pM_{\mathrm{sf}}\sqrt{(3p\varphi_{\mathrm{s}})^2+\left(\dfrac{2L_qT_e}{\varphi_{\mathrm{s}}}\right)^2}} \tag{4}$$

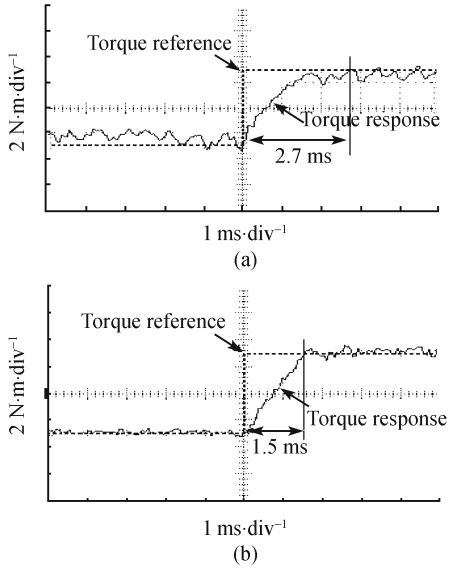


**Fig. 10** Experimental waveforms of the torque step response
(a) Basic DTC; (b) SVM-DTC

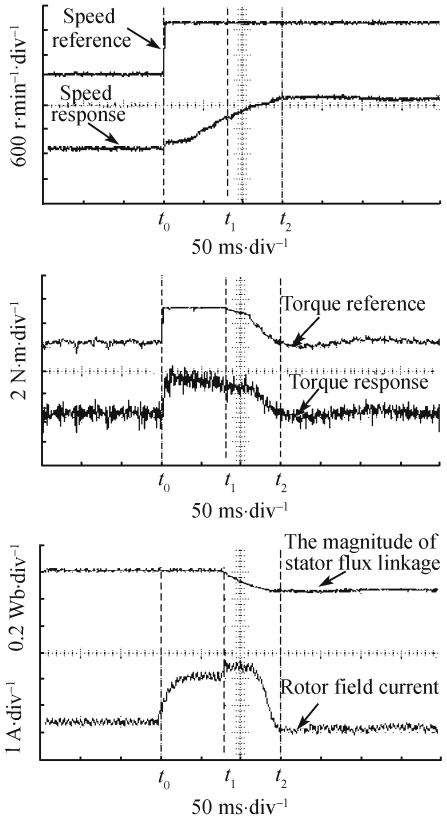


**Fig. 11** Field weakening operation

The given value of the rotor field current $i_f^*$ can be calculated from Eq. (4) when the given stator flux linkage $\varphi_s^*$ and the given torque $T_e^*$ are substituted in Eq. (4).

The experimental waveforms of weakening operation are shown in Fig. 11. The rotor speed begins increasing from point $t_0$ at 750 r/min. The speed is 1 500 r/min at point $t_1$ and the stator flux linkage begins reducing from 0.61 Wb as well as the torque with 3 N·m from this point. The rotor field current increases from 3 to 3.5 A at point $t_1$, from which the motor begins working in the weakening range. At point $t_2$, the speed is 2 000 r/min and the stator flux linkage is reduced to 0.45 Wb. The weakening operation is included in the SVM-DTC scheme well and the ESM works smoothly from the above experimental waveforms.

## 6 Conclusions

The SVM-DTC scheme also has advantages of the basic DTC, such as no rotation coordinate conversion and insensitiveness to motor parameter changes due to the only requirement of the stator resistance.

The SVM-DTC scheme substitutes the torque and the stator flux linkage hysteresis controllers of the basic DTC with the torque PI controller and one-step anticipation scheme of the stator flux linkage vector. Therefore, the ripples of the torque and the stator flux linkage are all reduced to a large degree.

The torque response time of the SVM-DTC drive is almost the same as that of the basic DTC.

The rotor field weakening scheme is still applied in the SVM-DTC drive, and the weakening operation is smoother and steadier.

**Acknowledgements** This work was supported by the Aeronautics Key Science Foundation of China (No. 98Z52001), the Fifteen Aeronautics Pre-research Item of China (No. 40200201).

## References

1. Zhong L, Rahman M F, Hu Y W, et al. Analysis of direct torque control in permanent magnet synchronous motor drives. IEEE Transactions on Power Electronics, 1997, 12(3): 528–535
2. Pyrhonen J, Niemela M, Kaukonen J, et al. Synchronous motor drives based on direct flux linkage control. Proceedings of the European Power Electronics Conference, 1997, (1): 434–439
3. Pyrhonen J, Niemela M, Kaukonen J, et al. Test results with the direct flux linkage control of synchronous motors. IEEE AES Systems Magazine, 1998, (4): 23–27
4. Casadei D, Serra G, Tani A. Constant frequency operation of a DTC induction motor drive for electric vehicle. Proceedings of ICEM, 1996, (3): 224–229
5. Xu L, Fu M. A novel sensorless control technique for permanent magnet synchronous motors (PMSM) using digital signal processor (DSP). Proceedings of Aerospace and Electronics Conference, 1997, (1): 403–406
6. Tang L X, Zhong L M, Rahman M F, et al. A novel direct torque controlled interior permanent magnet synchronous machine drive with low ripple in flux and torque and fixed switching frequency. IEEE Transactions on Power Electronics, 2004, 19(2): 346–354
7. Zhou Yangzhong, Hu Yuwen, Tian Jiao. Research of torque controller with variable proportion in permanent magnet synchronous motor drive. Proceedings of the CSEE, 2004, 24(9): 204–208 (in Chinese)
8. Baader U. High dynamic torque control of induction motor in stator flux oriented coordinates. ETZ Arch, 1998, 11(1): 11–17

9. Habetler T G, Profumo F, Pastorelli M, et al. Direct torque control of induction motor using space vector modulation, IEEE Transactions on Industry Applications, 1992, 28(5): 1 045–1 053
10. Wang Huangang, Xu Wenli, Li Jian, et al. A new approach to direct torque control of induction machines. Proceedings of the CSEE, 2004, 24(1): 107–111 (in Chinese)
11. Sun Xiaohui, Zhang Zengke, Han Zengjin. Research on torque ripple minimum of inductance motor based on direct torque control. Proceedings of the CSEE, 2002, 22(8): 109–112 (in Chinese)
12. Qian Kun, Xie Shousheng, Gao Meiyan, et al. Improved direct torque control method for induction motor applications. Proceedings of the CSEE, 2004, 24(7): 210–214 (in Chinese)
13. Yuan Dengke, Tao Shenggui. An improved scheme of the direct torque control system of induction motor. Proceedings of the CSEE, 2005, 25(8): 151–155 (in Chinese)
14. Lascu C, Andrzej M T. Combining the principles of sliding mode, direct torque control, and space-vector modulation in a high-performance sensorless ac drive. IEEE Transactions on Industry Applications, 2004, 40(1): 170–177
15. Zhou Yangzhong, Hu Yuwen, Huang Wenxin, et al. Effect of damper windings on the dynamic performance of electrically excited synchronous motor based on direct torque control. Acta Aeronautica et Astronautica Sinica, 2005, 26(4): 476–481 (in Chinese)